Processing and Characterization of Recycled Poly(ethylene terephthalate) Blends With Chain Extenders, Thermoplastic Elastomer, and/or Poly(butylene adipate-*co*-terephthalate)

Yottha Srithep,[1] Alireza Javadi,[2] Srikanth Pilla,[3] Lih-Sheng Turng,[1] Shaoqin Gong,[2] Craig Clemons,[4] Jun Peng[5]

[1] *Polymer Engineering Center, Department of Mechanical Engineering, University of Wisconsin-Madison, Madison, Wisconsin*

[2] *Department of Biomedical Engineering, University of Wisconsin-Madison, Madison, Wisconsin*

[3] *Department of Civil and Environmental Engineering, Stanford University, Stanford, California*

[4] *Forest Products Laboratory, USDA Forest Service, Madison, Wisconsin*

[5] *South China University of Technology, Guangzhou, China*

Poly(ethylene terephthalate) (PET) resin is one of the most widely used thermoplastics, especially in packaging. Because thermal and hydrolytic degradations, recycled PET (RPET) exhibits poor mechanical properties and lacks moldability. The effects of adding elastomeric modifiers, chain extenders (CE), and poly(butylene adipate-*co*-terephthalate), PBAT, as a toughener to RPET on its moldability and mechanical property were investigated. Melt blending of RPET with CE, thermoplastic elastomer (TPE), and/or PBAT was performed in a thermokinetic mixer (K-mixer). The blended materials were then injection molded to produce tensile specimens. Various techniques were used to study the mechanical properties, rheological properties, compatibility, and crystallization behavior of the RPET blends. By melt blending with proper additives, recycled PET regained its moldability, thereby enabling the recycling of RPET. Furthermore, the addition of CE greatly enhanced the mechanical properties of RPET. While the RPET and TPE blends also showed improved mechanical properties, the improvement was less significant and the blends were often immiscible due to the difference in polarities between RPET and TPE. Finally, it was found that the mechanical properties of RPET blends depended on the prior thermal history of the material and could be improved with an extra annealing step that increased the degree of crystallinity. POLYM. ENG. SCI., 51:1023–1032, 2011. **© 2011 Society of Plastics Engineers**

INTRODUCTION

Poly(ethylene terephthalate) (PET) is one of the most widely used thermoplastic polyesters. PET is extensively used in various applications, such as beverage bottles, fibers, moldings, and sheets because of its superior chemical, physical, mechanical, and (oxygen and carbon dioxide) barrier properties. The largest application of PET in the United States is the manufacturing of bottles [1], which has grown approximately 9% annually, from 1995 to 2007 [2]. Most of these beverage bottles are disposable, which inevitably raises environmental concerns over their waste. Thus, to lessen the environmental hazards and burdens created by disposing of PET in landfills, much of the post-consumer PET is recycled to be reused in certain applications. However, recycled PET (RPET) undergoes hydrolytic and thermal degradations which lead to a reduction in the molecular weight and intrinsic viscosity that, in turn, deteriorates the mechanical properties and moldability of the recycled material [3–8]. Hydrolytic reactions, which are caused by retained moisture and

Correspondence to: Lih-Sheng Turng; e-mail: turng@engr.wisc.edu or Shaoqin Gong; e-mail: sgong@engr.wisc.edu

Contract grant sponsor: Wisconsin System Solid Waste Research Program, Thai Government.

DOI 10.1002/pen.21916

Published online in Wiley Online Library (wileyonlinelibrary.com).

© 2011 Society of Plastics Engineers

contaminants, result in chain scission with carboxylic acid and hydroxyl ester end groups (cf. Fig. 1a), whereas the thermal cleavage of the PET ester bond leads to the formation of carboxylic end groups and vinyl esters (cf. Fig. 1b) [9].

The property deterioration of RPET may be compensated for by the addition of reinforcing fillers and toughening modifiers. For example, PET has been blended or compounded with several polymers, fillers, and nanoparticles to modify its physical properties. The addition of a second component to improve mechanical performance has been reported [10–13].

PET has also been blended with various elastomers such as ethylene propylene rubber (EPR), ethylene propylene diene monomer rubber (EPDM), nitrile butadiene rubber (NBR), and styrene-butadiene rubber (SBR) [14–21]. Because of the difference in their polarities, these blends are often immiscible resulting in unfavorable mechanical properties. It has been observed that the incorporation of suitable compatibilizer agents is essential to establish an optimal level of interaction between RPET and the elastomer components. On the other hand, adding certain chain extenders (CE) is an effective way to increase the molecular weight (and thus melt viscosity) of PET. In general, chain extenders are low-molecular-weight, multifunctional compounds capable of a rapid reaction with the polymer end groups, leading to the coupling of macromolecules. Various organic substances, such as diepoxides, diisocyanates, dianhydrides, carbodiimides, and bisoxazolines, have been used to extend PET chains [8, 9, 22]. Combining RPET with other polymers, such as PBAT, can also improve properties such as toughness. This study investigates the effects of adding CE (chain extenders), TPE (thermoplastic elastomer), and PBAT (poly(butylene adipate-*co*-terephthalate)), on the mechanical, morphological, rheological, and thermal properties of RPET. Various characterization techniques including tensile testing, dynamic mechanical analysis, impact testing, rheological analysis, scanning electron microscopy, and differential scanning calorimetry were used. The effects of prior thermal history and an extra annealing step on the properties of the injection-molded RPET blends will also be presented.

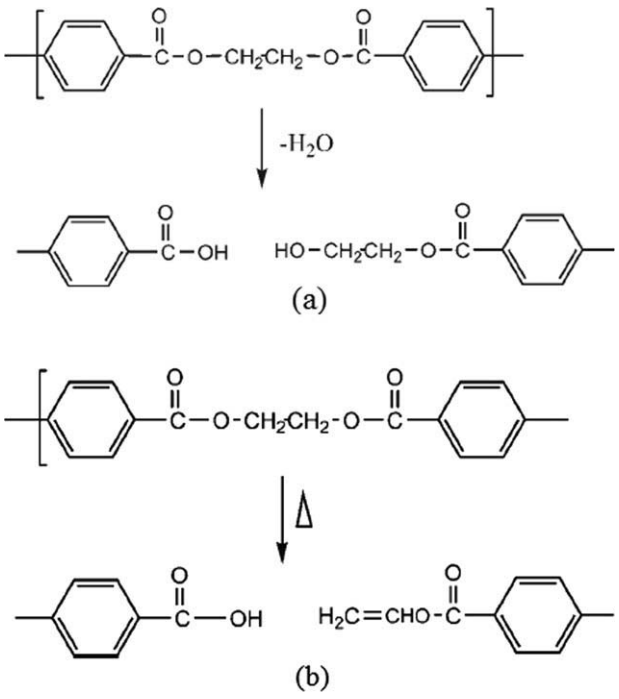

FIG. 1. (a) Hydrolytic and (b) thermal degradation reactions of PET.

EXPERIMENTS

Materials

Scraps and pelletized RPET (PET-H.S.3915.90 clear plastic flake of 9.525 mm or 3/8 inches from 2-l soda bottles) were received from Merlin Plastics Alberta Inc. The RPET was chemically stable and resistant to attack by oils, weak acids, and weak alkalis. The melting temperature (T_m) was 245°C and the measured melt flow index (MFI) is 30 g/10 min and 60 g/10 min (weight 2.16 kg) at 260°C and 270°C, respectively. Thermoplastic elastomer with a density of 0.93 g/cm^3 (TPE, Santoprene 8211-45) was purchased from ExxonMobil Chemical. The TPE, also called thermoplastic dynamic vulcanizate (TPV), is an alloy between ethylene propylene diene monomer (EPDM) rubber and polypropylene (PP) with the rubber particles dispersed in the PP phase. Chain extender (CE, CESA-Extend 9930C) was supplied by Clariant Masterbatches. The chain extender is an epoxy-functional styrene acrylic copolymer (oligomeric coupling agent) that has functional group (—R—COO—R) that may be added to degraded condensation polymers to relink polymer chains broken by thermal, oxidative, or hydrolytic degradation. Poly(butylene adipate-*co*-terephthalate (PBAT), a commercialized aliphatic-*co*-aromatic biodegradable and flexible copolymer and toughening agent, was purchased from BASF Corporation under the commercial name Ecoflex®.

Processing

The RPET was combined with CE, TPE, and/or PBAT in a variety of formulations (Table 1). RPET was dried in an oven for 10 h at 110°C before processing. Prior to injection molding, materials were melt compounded using a thermokinetic mixer (K-mixer). They were compounded in 200 g batches and discharged when the temperature reached 260°C. There was no external heating source for blends in the K-mixer besides frictional (viscous) heat, and the compounding process was completed in less than 2 min. This short heating/mixing time reduces the potential for further thermal degradation. The K-mixer's rotor

 DOI 10.1002/pen

TABLE 1. Percent composition (by weight) of the materials compounded.

No.	Sample	RPET (%)	CESA-Extend 9930C (%)	PBAT (%)	Thermoplastic elastomer (TPE) (%)
1	RPET + 1.3% CE	98.7	1.3	0	0
2	RPET + 25% PBAT + 1.3% CE	73.7	1.3	25	0
3	70% RPET + 30% TPE	70	0	0	30
4	50% RPET + 50% TPE	50	0	0	50
5	TPE	0	0	0	100

speed was 4000 rpm. After discharge, the molten blend was pressed into a flat sheet and subsequently granulated. Tensile bars (ASTM D638) were injection molded using a Boy 22S (PA, USA) injection molding machine. Solid tensile bars were molded at the processing conditions shown in Table 2.

Differential Scanning Calorimetry

A differential scanning calorimeter (DSC 200 PC Phox®) was used to study the properties of the blended materials. Specimens of 4–5 mg were placed in aluminum sample pans and heated from 25 to 270°C at a 10°C/min heating rate and held for 5 min at 270°C to erase any prior thermal history before cooling at 10°C/min to 25°C. The specimens were then reheated to 270°C and cooled down to room temperature using the same heating and cooling rates of 10°C/min. The crystallization temperature (T_c), melting temperature (T_m), apparent melting enthalpy (ΔH_f), and enthalpy of cold crystallization (ΔH_{cc}) were determined from DSC curves. Parameters T_m and ΔH_f were taken as the peak temperature and the area of the melting endotherm, respectively.

The absolute degree of crystallinity (χ_c) of the RPET phase was calculated by

$$\chi_c(\%) = \frac{\Delta H_f(\text{RPET})}{\Delta H^\circ(\text{RPET})} \times \frac{100}{w} \quad (1)$$

TABLE 2. Injection molding conditions used to mold the ASTM tensile bars.

Mold temperature (°C)	46
Nozzle temperature (°C)	260
Injection speed (cm^3/s)	14
Packing pressure (bar)	90
Packing time (s)	10
Screw (RPM)	35
Cooling time (s)	20

where ΔH°(RPET) is the enthalpy of melting per gram of 100% crystalline (perfect crystal) (120 J/g) and w is the weight fraction of RPET in the blend [9].

To determine the original crystallinity of the injection molded sample that was subjected to rapid cooling during the molding process, the extra heat released by the amorphous phase forming crystallites during heating (i.e., enthalpy of cold crystallization) was subtracted from the total endothermic heat flow due to the whole crystallites. Thus, the modified equation for the original crystallinity of the injection molded sample can be written as follows:

$$\chi_c(\%\ \text{Crystallinty}) = \frac{\Delta H_f(\text{RPET}) - \Delta H_{cc}(\text{RPET})}{\Delta H^\circ(\text{RPET})} \times \frac{100}{w} \quad (2)$$

Mechanical Testing

Tensile and notched Izod impact tests were performed on the injection molded samples following the ASTM-D-638-02 and ASTM-D-256-02 standards, respectively. The static tensile modulus, strength, and strain-at-break were measured at room temperature (~25°C) and atmospheric conditions (relative humidity of ~50% ± 5%) on an MTS Sintech-10/GL mechanical testing instrument. Additional tensile tests were performed on the molded tensile bars after the specimens went through an annealing step in an oven. That is, the tensile bars were placed in an oven and heated from 25 to 185°C at a rate of 5°C/min and then cooled to room temperature before the test. The tensile testing was performed on all specimens using an initial load of 0.5 N and a constant crosshead speed of 12.7 mm/min (0.5 in/min).

Prior to impact testing, rectangular specimens approximately 63.5 mm × 12.7 mm × 3.2 mm were cut from injection molded parts. The notched specimens were conditioned at (25°C and a relative humidity of 50% ± 5%. Five specimens of each sample group were tested, and the average results were reported.

Dynamic Mechanical Analysis

Dynamic mechanical analysis (DMA) measurements were performed on an RSAIII DMA instrument in three-point bending mode. The dimensions of the rectangular specimen were about 17.6 mm × 12.7 mm × 3.2 mm, which were cut from injection-molded parts. During the DMA test, the specimens were heated at a rate of 3°C/min from −45°C to 185°C with a frequency of 1 Hz and a strain of 0.01%, which is in the linear viscoelastic region, as determined by a strain sweep. Additional specimens were tested after first being subject to the same heating cycle without sinusoidal deformation in an oven. That is, the specimens were placed in an oven and heated from −45°C to 185°C at 3°C/min, akin to the heating scan used in the DMA test, then cooled to room tempera-

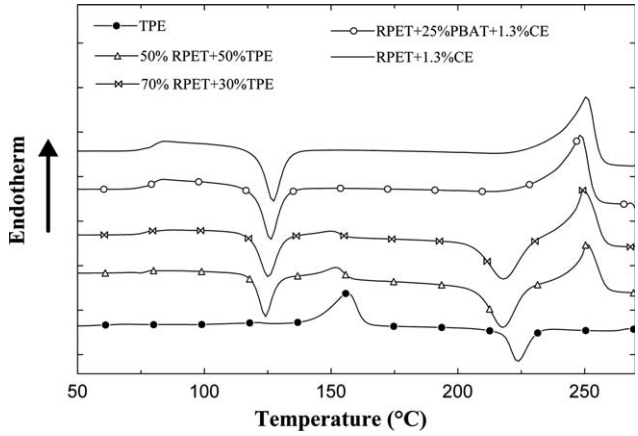

FIG. 2. Melting curves of the PET blends. Data obtained from the first heating cycle.

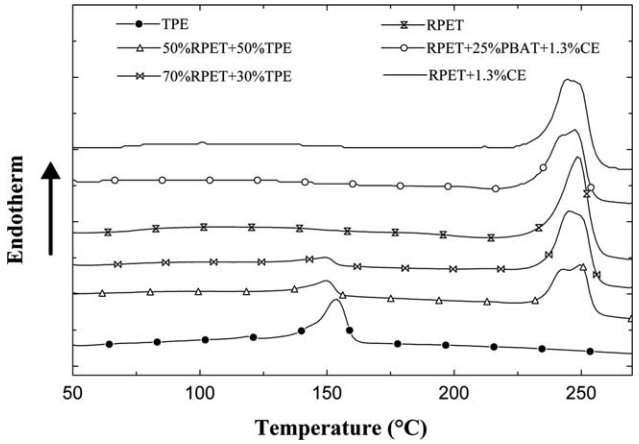

FIG. 3. Melting curves of the RPET blends. Data obtained from the second heating cycle.

ture before DMA testing. Similar to that in the tensile testing, the purpose of the extra heating cycle prior to the test is to find out the effect of annealing on the dynamic mechanical properties of the molded RPET blend specimens.

Rheological Properties

The shear viscosities of the polymer blends compounded in this study were measured over a range of shear rates using a TA Instruments ARES-LSII rheometer with a parallel plate geometry (plate radius = 25 mm; gap = 3.5 mm). Disks of proper sizes were cut from the tensile bars and then inserted between the plates and brought to the testing temperature and gap thickness. Steady shear tests were made at 260°C under a nitrogen gas purge to avoid thermo-oxidative degradation.

Scanning Electron Microscopy

The fractured surfaces were examined using an scanning electron microscopy (SEM; LEO 1530) operated at 3 kV. The samples obtained from the tensile bars were cryogenically frozen in liquid nitrogen and then quickly impact-fractured. All specimens were sputter-coated with a thin layer of gold (~20 nm) prior to examination.

RESULTS AND DISCUSSION

Thermal Properties

Thermal properties of RPET blends, including crystallization and melting behaviors, were investigated using DSC. The thermograms (solid curves) for the five material compositions are listed in Table 1, and the numerical values of temperatures obtained from the first and second heating cycles are plotted in Figs. 2 and 3. The cooling run is shown in Fig. 4. The corresponding thermal data are listed in Table 3. The data obtained from the first heating cycle include the effect of the prior thermal history of the injection-molded samples, while the data obtained from the second heating cycle allow for a direct comparison of the crystallization behavior of different materials after erasing the thermal history through the first heating cycle.

First Heating Cycle. As shown in Fig. 2, TPE has one endothermic and one exothermic peak which occurred around 150 and 220°C, respectively. Recall that the TPE used in this study is an alloy between EPDM rubber and PP with the rubber particles dispersed in the PP phase. An endothermic peak at a temperature around 150°C resulted from the melting of the crystalline polymer (PP) and the exothermic peak at a temperature around 220°C is the vulcanization process in residual, nonvulcanized rubber, hence the material gave off some heat.

Also, Fig. 2 shows that two endothermic and two exothermic peaks were observed for RPET + TPE blends specimens (i.e., 70% RPET + 30% TPE and 50% RPET + 50% TPE). However, only one endothermic and one

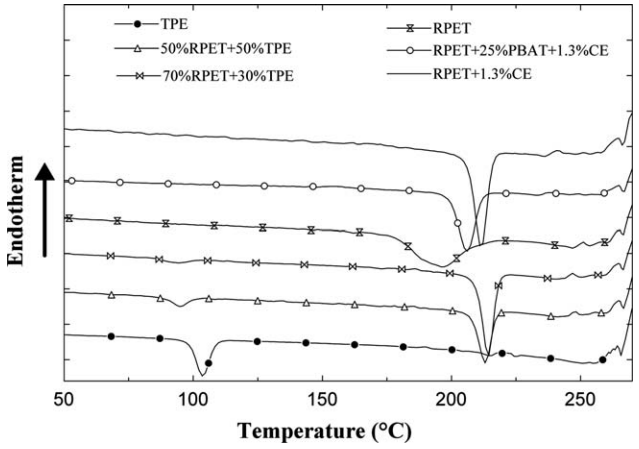

FIG. 4. Melting curves of the RPET blends. Data obtained from the cooling cycle.

 DOI 10.1002/pen

TABLE 3. Thermal characteristics of RPET blends.

Sample	RPET					TPE
	Cold crystallization		Melting		Degree of crystallinity	
	Temp (°C)	Enthalpy (J/g)	Temp (°C)	Enthalpy (J/g)	χ_c (%)	Endothermic peak (°C)
First heating						
RPET + 1.3% CE	126.75	–21.6	250.71	44	18.91	–
RPET + 25% PBAT + 1.3% CE	107.87	–14.57	248.66	43.01	32.15	–
70% RPET + 30% TPE	126.34	–18.64	250.71	30.86	14.33	149.74
50% RPET + 50% TPE	123.88	–13.31	251.53	21.21	13.16	150.56
TPE	–	–	–	–	–	155.9
Second heating						
RPET						
RPET + 1.3% CE	–	–	246.19	43.39	36.6	–
RPET + 25% PBAT + 1.3% CE	–	–	246.19	40.19	46.25	–
70% RPET + 30% TPE	–	–	246.6	34.74	28.95	149.74
50% RPET + 50% TPE	–	–	247	23.19	38.65	150.56
TPE	–	–	–	–	–	153.8

exothermic peak were shown for TPE, RPET + 1.3% CE and RPET + 25% PBAT + 1.3% CE specimens. The first exothermic peak for all RPET blend specimens (at a temperature range around 110–130°C) is referred to as the cold crystallization peak of RPET. The second exothermic peak (at a temperature of 220°C) corresponds to the vulcanization of TPE which occurred only with TPE blend specimens. Two exothermic peaks for RPET and TPE blends suggest that the two materials are immiscible. Recall that the specimens were taken from injection molded samples that underwent rapid cooling during the molding process, thereby impairing the crystallization process of the samples. Upon reheating during the DSC experiment, RPET molecules in the amorphous regions were able to rearrange and crystallize. With the addition of PBAT, the peak temperature of cold crystallization of RPET decreases. This indicates that the addition of PBAT promotes the onset of crystallization of the RPET material. The last peaks (at a temperature around 250°C) observed for all RPET blend specimens are the melting point of RPET. The shoulders around 60–80°C in the DSC thermograms in Fig. 2 reveal the glass transition temperature of the RPET blends.

Table 3 shows the numerical values of temperatures and enthalpies from the first heating curve of the RPET blends. The enthalpies of crystallization and melting peaks of RPET decreased as the amount of TPE increased. However, the enthalpies of the melting peak of the RPET was still somewhat constant compared to RPET + 1.3% CE as PBAT was added, indicating that there was enhanced RPET crystallization during cooling during the injection molding process. As a result, there was higher crystallinity.

Second Heating Cycle. Figure 3 and Table 3 show the thermograms and numerically analyzed data of the RPET blends, respectively, from the second heating cycle. Unlike the first heating cycle, no exothermic peaks were observed because the prior thermal history of the injection-molded samples was erased in the first heating cycle. Figure 3 shows that double endothermic peaks (at temperatures around 150°C and 245°C) were obtained for the blends of RPET and TPE due to the differences in the endothermic temperatures of the two materials. Moreover, Fig. 3 shows that there is only one melting peak at around the same temperature (around 245°C) for the RPET and the RPET + PBAT + CE blend, but the melting peaks of RPET were wider for all the blends. This indicates that the addition of CE and PBAT does not affect the melting temperature of RPET. Also, as in the case of the first heating cycle, the addition of PBAT increased the crystallinity of RPET and the degree of crystallinity of all samples was found to be higher than that obtained during the first heating cycle.

Cooling Cycle. Also as shown in Fig. 4, two exothermic peaks were observed for the RPET + TPE blend specimens (i.e., 70% RPET + 30% TPE and 50% RPET + 50% TPE). The first exothermic peak (at a temperature range around 95–105°C) corresponds to the crystallization of the PP phase in the TPE. The second endothermic peak (at a temperature of 190–220°C) is the crystallization peak of RPET. However, only one exothermic peak was shown for TPE, RPET + 1.3% CE, and RPET + 25% PBAT + 1.3% CE specimens. The exothermic peak of the TPE is associated with the crystallization of the PP phase in the TPE, whereas for the RPET + 1.3% CE and RPET + 25% PBAT + 1.3% CE specimens the peak is due to the crystallization of the RPET. The crystallization temperature of RPET alone was found to be lowest among all of the samples, suggesting that the presence of other materials (e.g., PBAT or CE) as additives facilitated the crystal nucleation process and resulted in a higher crystallization temperature. Two exothermic peaks for RPET and TPE indicate that the two materials are immiscible.

TABLE 4. Mechanical properties of RPET blends.

Sample	Ultimate tensile strength (MPa)	Tensile modulus (MPa)	Strain at break	Impact strength (kJ/m^2)
RPET + 1.3% CE	53.2 ± 3.08	1450.3 ± 105.05	NB[a]	3.89 ± 0.028
RPET + 25% PBAT + 1.3% CE	39.4 ± 0.78	1181.1 ± 124.40	NB	5.17 ± 0.025
70% RPET + 30% TPE	18.9 ± 0.43	773.3 ± 62.33	0.1 ± 0.02	3.33 ± 0.005
50% RPET + 50% TPE	5.9 ± 0.39	264.7 ± 35.60	0.115 ± 0.07	1.83 ± 0.005
TPE	1.26 ± 0.02	2.83 ± 0.26	NB	NB
Heat treated sample				
RPET + 1.3% CE	62.6 ± 9.3	1746.7 ± 1.57	0.05 ± 0.01	–
RPET + 25% PBAT + 1.3% CE	47.8 ± 0.01	1281.8 ± 11.22	0.23 ± 0.02	–
70% RPET + 30% TPE	21.63 ± 0.3	884.8 ± 24.6	0.0544 ± 0.002	–
50% RPET + 50% TPE	1.44 ± 0.1	309.7 ± 0.1	0.02 ± .01	–

[a] NB, not broken.

Tensile and Impact Properties

Tensile tests (according to ASTM-D-638-02) were performed on the injection molded specimens of the RPET blends. Properties such as tensile modulus, tensile strength, and strain at break were measured as shown in Table 4. The representative stress–strain curves are featured in Fig. 5. As can be seen in Table 4 and Fig. 5, RPET + 1.3% CE and RPET + 25% PBAT + 1.3% CE specimens were not broken at the preset maximum strain. The strain-at-break of RPET blended with TPE became higher as the amount of TPE increased, but their strength and modulus were lower than those of PET blended with CE and PBAT. The strain at break of 70% RPET + 30% TPE and 50% RPET + 50% TPE was found to be 0.1 and 0.115, respectively. The less than desired strain at break and mechanical properties of the RPET + TPE blends were probably due to the difference in the polarities between RPET and TPE.

As shown in Table 4 and Fig. 5, the RPET with 1.3% CE had the highest value of ultimate tensile strength, which was 53.2 MPa. For the RPET + 25% PBAT + 1.3% CE with a 25% increase in the PBAT the ultimate tensile strength decreased to 39.4 MPa. The tensile strengths for 70% RPET + 30% TPE and 50% RPET + 50% TPE were found to be 18.9 MPa and 5.9 MPa, respectively. A similar trend was observed for the tensile modulus. The RPET with 1.3% CE had the highest value of ultimate tensile modulus following by RPET + 25% PBAT + 1.3% CE, 70% RPET + 30% TPE, and 50% RPET + 50% TPE.

Figure 6 represents the tensile test results of the RPET blends after subjecting them to an annealing step-slow heating from room temperature to 185°C, which is higher than the cold crystallization temperature of RPET, and then cooled to room temperature-before the test. Properties such as tensile modulus, tensile strength, and strain at break were also measured as shown in Table 4. As can be seen in Table 4 and Fig. 6, the tensile modulus and tensile strength of the RPET blends were noticeably higher due to RPET recrystallization and became stronger and stiffer. RPET + 1.3% CE still had the highest value of ultimate tensile strength and tensile modulus, which was 62.6 MPa and 1746.7 ± 1.57 MPa, respectively. However, both RPET + 1.3% CE and RPET + 25% PBAT + 1.3% CE samples were broken and all tensile bars were broken at a strain-at break lower than that of the untreated

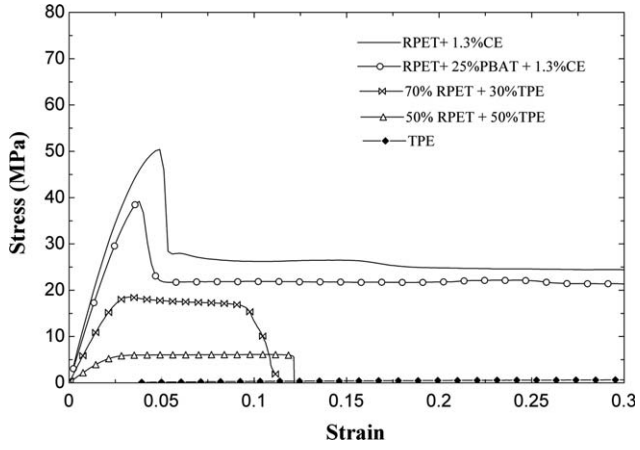

FIG. 5. Tensile stress versus strain curves for the TPE and RPET blends.

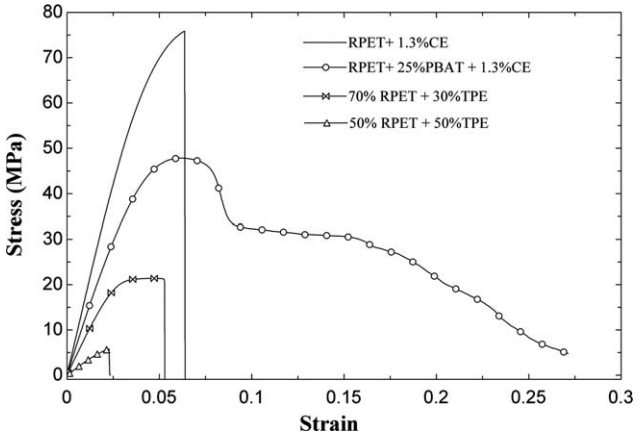

FIG. 6. Tensile stress versus strain curves for the RPET blends after heat treatment.

 DOI 10.1002/pen

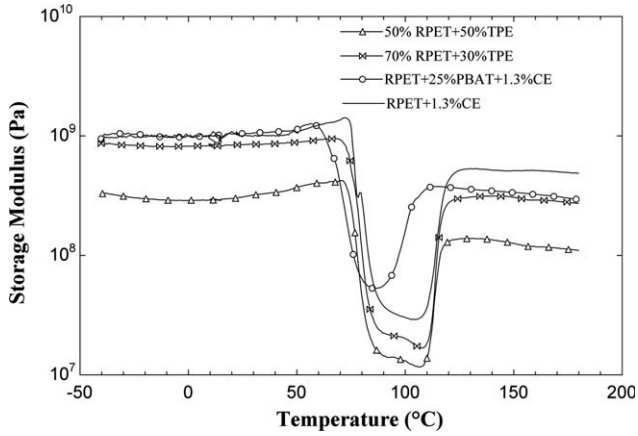

FIG. 7. Storage moduli of the RPET blends for specimens cut directly from injection molded tensile test bars.

samples, which indicated that the ductility of the treated specimens was reduced. The strain-at-break of 50% RPET + 50% TPE was lowest at 0.02 ± 0.01.

The impact strengths of the four RPET blends and TPE are also shown in Table 4. As can be observed, the blend containing 50% RPET and 50% TPE exhibited the lowest impact strength among the RPET blends. Also shown in the Table 4 is the addition of chain extenders (CE) that lead to a higher impact strength, which is about double the impact strength of the 50% RPET + 50% TPE. Nonetheless, all of these blends performed much better than the RPET alone, which is brittle and difficult to mold, let alone being tested for impact strength [23].

In general, RPET with chain extenders was found to have higher mechanical properties. This might be due to the fact that the chain extenders react and rejoin the broken chains of the hydroxyl (—OH) functional group or carboxyl (—COOH) end groups of PET during melt processing, thus leading to an increase in the blend's tensile strength and modulus [23], while RPET with TPE gave lower mechanical properties. The reason for the lower mechanical properties resulted from an incompatibility between the RPET and TPE [14]. Finally, after the RPET blend specimens were reheated beyond the cold-crystallization temperature, they became stronger but had a lower strain-at-break.

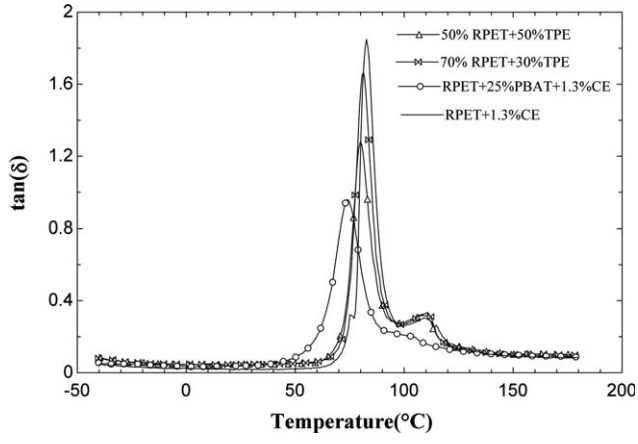

FIG. 8. Tan-δ curves of the RPET blends.

Dynamic Mechanical Properties

The viscoelastic properties of the RPET blends were studied using DMA. The resulting storage moduli and glass transition temperatures in terms of tan-δ of all of the RPET blends are shown in Figs. 7 and 8, respectively. Note that the storage moduli of all of the specimens decreased rapidly between 60 and 80°C (Fig. 7) due to the glass transition temperature of RPET [24] (cf. Fig. 8). Between 90 and 110°C, their moduli started to increase, which corresponds to the range of the cold crystallization temperature of RPET (cf. Fig. 2). The increase in crystallinity during cold crystallization increases the rigidity of the specimen. Since the RPET + 25% PBAT + 1.3% CE has the lowest cold crystallization temperature (cf. Fig. 2), the transitions in storage modulus and glass transition temperature also occur at the lowest temperature. The storage modulus of 50% RPET + 50% TPE was the lowest, and RPET + 1.3%CE was the highest at high temperature. While the glass transition of the blends can be easily identified by the peaks in the tan-δ curves in Fig. 8, one can also see a weak transition appeared at about 115°C, which is assigned to the cold crystallization temperatures of RPET [24]. Note that the T_g of the PET-PBAT blend is lower than that of the RPET-TPE and RPET-CE blends at around 73.6°C and the T_g of the RPET + 1.3% CE is highest at around 82.9°C. Table 5 tabulates the glass transition temperatures of the various RPET blends based on the tan-δ curves.

Figure 9 presents the DMA results of the specimens with an additional heat treatment by subjecting them to the same DMA thermal history (i.e., heating at a rate of 3°C/min from −45 to 185°C) without loading. Interestingly, the substantial drop in the storage moduli previously shown in Fig. 7 disappeared with the new test specimens. This suggests that the extra "annealing process" allowed the cold crystallization process to occur prior to DMA testing. For the new DMA tests, only a small declining trend was observed for the storage moduli of all specimens as the temperature increased with the most rapid reduction occurring at the glass transition region. In the glassy region

TABLE 5. Glass transition temperatures of RPET blends.

No.	Sample	Glass transition temperature (°C)	Glass transition temperature (°C) (heat treated sample)
1	RPET + 1.3% CE	82.9	98.7
2	RPET + 25% PBAT + 1.3% CE	73.6	93.6
3	70% RPET + 30% TPE	81.6	99.7
4	50% RPET + 50% TPE	79.6	101.5

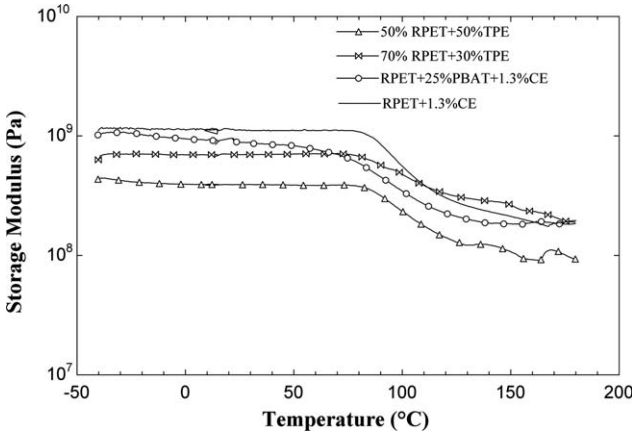

FIG. 9. Storage moduli of the RPET blends after heat treatment.

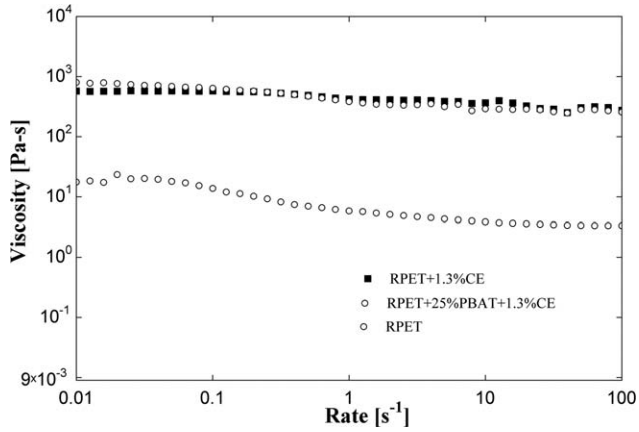

FIG. 11. Flow curves for RPET-CE and PET-PBAT-CE blends ($T = 260°C$).

(<60°C), the storage modulus of the specimen is highest when PET was blended with 1.3% CE. The addition of 25% PBAT decreased the storage modulus, but it was still higher than that of the RPET and TPE blends.

In the glass transition region, two crossovers were observed between the RPET +1.3% CE, RPET + 25% PBAT + 1.3% CE, and 70% RPET + 30% TPE because of the glass transition of RPET. Above the glass transition region, the storage moduli of all specimens continued to decrease with increasing temperature.

The temperature dependence of the tangent (tan-δ) of the blends after the heat treatment is presented in Fig. 10. The glass transition temperature (T_g) is obtained from the peaks of the tan-δ curves. Note that the glass transition temperatures increase slightly compared to those of the specimens without the heat treatment. In particular, the T_g of the RPET-PBAT blend is lower than that of the RPET-TPE and RPET-CE blends at around 93.6°C and the T_g of 50% RPET + 50% TPE is highest at around 101.5°C due to the fact that the material had the lowest amount of RPET. Table 5 tabulates the new glass transition temperatures of the various RPET blends based on the tan-δ curves.

Rheological Properties

The modification of the molecular structure during processing is reflected in the rheological characteristics of the RPET samples. A significant increase in viscosity due to the addition of CE in RPET is evident from the log–log viscosity–shear rate curves reported in Fig. 11. Furthermore, there is only a minor difference in the shear viscosity between the RPET + 1.3% CE and the RPET + 25% PBAT + 1.3% CE. This significant increase in viscosity suggests that the CE increased the molecular weight of the RPET; namely, the CE rejoins the broken chains of the hydroxyl or carboxyl end groups [23].

Figure 12 shows a plot of log–log shear viscosity for RPET blended with TPE as a function of shear rate. At low shear rates, the TPE's viscosity is about 10^5 Pa s, while RPET's viscosity is about 10^1 Pa s. The shear viscosity of RPET shows only a very slight decrease with increasing shear rate initially and then almost behaves like a Newtonian fluid, suggesting a much reduced molecular weight resulting from the degradation. For the case of RPET + TPE, as the amount of TPE material is increases, the

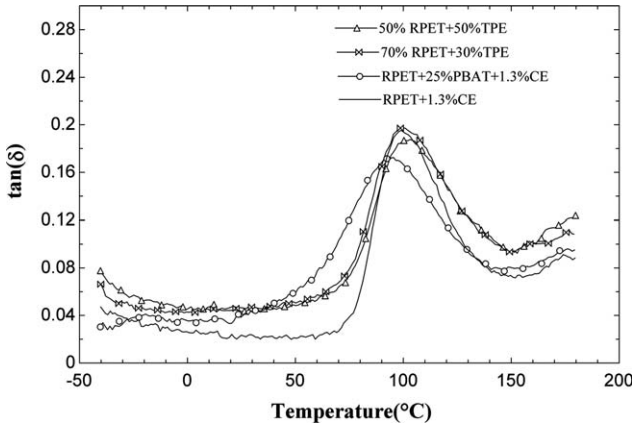

FIG. 10. Tan-δ curves of the RPET blends after heat treatment.

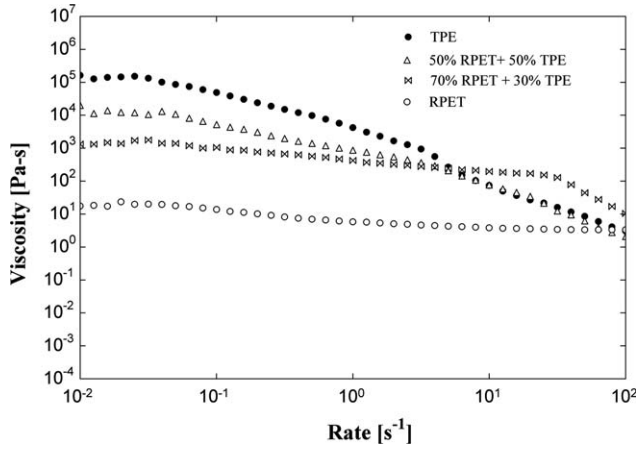

FIG. 12. Viscosity of RPET, TPE, and RPET + TPE blends.

 DOI 10.1002/pen

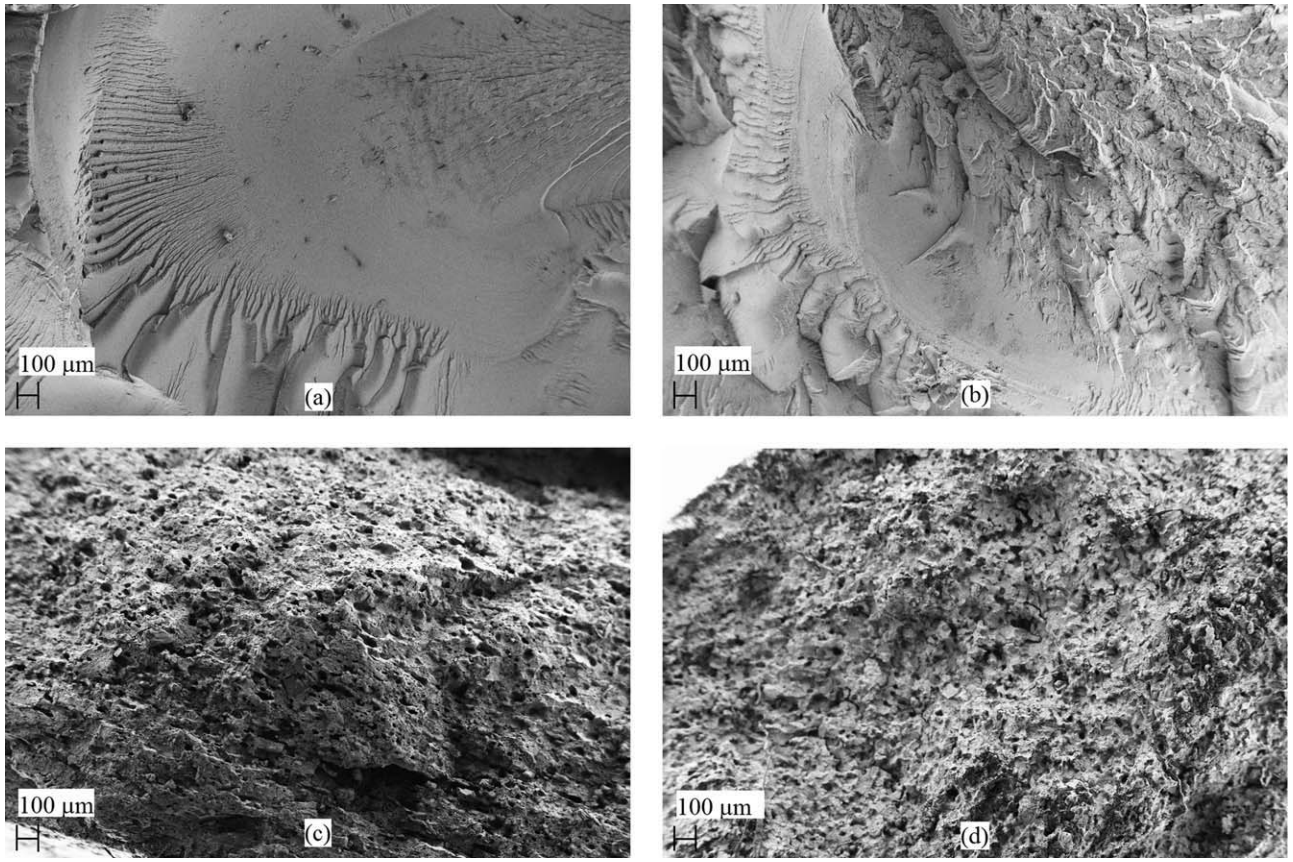

FIG. 13. SEM images of (a) RPET + 1.3% CE, (b) RPET + 25% PBAT + 1.3% CE, (c) 70% RPET + 30% TPE, and (d) 50% RPET + 50% TPE.

viscosity increases and becomes more like TPE. Shear thinning behavior can also be observed in these curves, especially with TPE and PET + TPE blends.

Fracture Surface Analysis via SEM

Figure 13 shows representative SEM images of RPET blends. All images were taken at the same magnification (scale bar: 100 μm). These SEM images provide information on the microstructure and the fracture behavior of the specimens. The fracture surfaces of the PET + CE and PET + PBAT + CE blends are rather smooth and suggest brittle fracture after cryogenic freezing, whereas the blends of RPET and TPE show some small cavities. The reason for the formation of these cavities in the blends is probably due to the volatile compounds released during vulcanization in the TPE phase that contribute to the weight reduction. The tensile bars of PET + 1.3% CE, RPET + 25% PBAT + 1.3% CE, 70% PET + 30% TPE, and 50% PET + 50% TPE weighed about 9.4, 9.2, 8.34, and 7.52 g, respectively.

CONCLUSION

The mechanical properties of RPET can be improved by the addition of chain extenders (CE), and poly(butylene adipate-co-terephthalate) (PBAT), or thermoplastic elastomer (TPE). The storage moduli of the injection molded RPET blends at elevated temperatures (i.e., above the glass transition temperature) can also be enhanced through an annealing process that increases the degree of crystallinity although the materials would have lower strain-at-break. More importantly, the enhanced moldability also allows them to be easily molded via injection molding, thereby enabling the recycling of PET for a host of applications. By adding chain extenders, the molecular weight of RPET increases, as does its viscosity and mechanical properties. Even though adding TPE enhances the moldability, RPET and TPE are immiscible, thus limiting the improvements in mechanical properties. Compatibilizers are needed to improve the mechanical properties of the blends.

REFERENCES

1. R. Hernandez, S.E.M. Selke, J. Culter, and J.D. Culter, *Plastics Packaging: Properties, Processing, Applications, and Regulations*, Hanser Gardner Publications, Cincinnati, OH (2000).
2. K. Dongho, *An Exploration into the Use of Stepwise Regression Analysis to Determine Post-Consumer Recycled PET Content in PET Sheet*, Michigan State University (2009).

3. Y. Zhang, W.H. Cuo, H.S. Zhang, and C.F. Wu, *Polym. Degrad. Stabil.*, **94**, 7 (2009).
4. L.H. Buxbaum, *Angew. Chem. Int. Ed.*, **7**, 3 (1968).
5. W. Schnabel, *Polymer Degradation: Principles and Practical Applications*, MacMillan Publishing Company, New York (1982).
6. N. Grassie and G. Scott, *Polymer Degradation and Stabilization*, Cambridge University Press (1985).
7. N. Cardi, R. Po, G. Giannotta, E. Occhiello, F. Garbassi, and G. Messina, *J. Appl. Polym. Sci.*, **50**, 9 (1993).
8. N. Torres, J. Robin, and B. Boutevin, *Eur. Polym. J.*, **36**, 10 (2000).
9. P. Kiliaris, C.D. Papaspyrides, and R. Pfaendner, *J. Appl. Polym. Sci.*, **104**, 3 (2007).
10. M. Canetti and F. Bertini, *Compos. Sci. Technol.*, **67**, 15 (2007).
11. K. Friedrich, M. Evstatiev, S. Fakirov, O. Evstatiev, M. Ishii, and M. Harrass, *Compos. Sci. Technol.*, **65**, 1 (2005).
12. C. Fuchs, D. Bhattacharyya, and S. Fakirov, *Compos. Sci. Technol.*, **66**, 16 (2006).
13. J.J. Hernández, M.C. García-Gutiérrez, A. Nogales, D.R. Rueda, and T.A. Ezquerra, *Compos. Sci. Technol.*, **66**, 15 (2006).
14. P. Phinyocheep, I. Saelao, and J.Y. Buzare, *Polymer*, **48**, 19 (2007).
15. D.E. Mouzakis, N. Papke, J.S. Wu, and J. Karger-Kocsis, U.S. Patent 00,218,995 (2000).
16. N. Papke and J. Karger-Kocsis, *Polymer*, **42**, 3 (2001).
17. W. Loyens and G. Groeninckx, *Polymer*, **43**, 21 (2002).
18. W. Loyens and G. Groeninckx, U.S. Patent 10,221,352 (2002).
19. S. Al-Malaika and W. Kong, *Polymer*, **46**, 1 (2005).
20. A. Sánchez-Solís, F. Calderas, and O. Manero, *Polymer*, **42**, 7335 (2001).
21. K.L. Fung and R.K.Y. Li, *Polym. Test.*, **24**, 863 (2005).
22. A.A. Haralabakopoulos, D. Tsiourvas, and C.M. Paleos, *J. Appl. Polym. Sci.*, **71**, 13 (1999).
23. X.W. Tang, W.H. Guo, G.R. Yin, B.Y. Li, and C.F. Wu, *J. Appl. Polym. Sci.*, **104**, 4 (2007).
24. Y. Zhang, H.S. Zhang, Y.B. Yu, W.H. Guo, and C.F. Wu, *J. Appl. Polym. Sci.*, **114**, 2 (2009).

 DOI 10.1002/pen